Fluidization by Lift

Daniel D. Joseph
Department of Aerospace Engineering and Mechanics
107 Akerman Hall, 110 Union Street SE
University of Minnesota
Minneapolis, MN 55455

(612) 625-0309 office; (612) 625-1558 fax

E-mail: *joseph@aem.umn.edu*

World Wide Web: *http://www.aem.umn.edu/Solid-Liquid_Flows*

Abstract

Our modeling focuses on the problem of fluidization by lift of single particles, many particles and very many small particles in shear flows. Fluidization by lift (slurries) is different and less well understood than fluidization by drag (fluidized beds). In commercial packages for slurry flow in pipes, conduits and fractured oil and gas reservoirs, the all important lift forces are not modeled, and in academic studies they are not modeled well.

The theory of lift is one of the great achievements of aerodynamics. Airplanes take off, rise to a certain height, and move forward under a balance of lift and weight. The lift and suspension of particles in the flow of slurries is another application in which lift plays a central role; in the oil industry we can consider the removal of drill cuttings in horizontal drill holes and sand transport in fractured reservoirs. The theory of lift for these particle applications is undernourished and in most simulators no lift forces are modeled. Models of lift must be based on empirical data ultimately from experiments. A more systematic and analytical way to generate empirical data is by direct numerical simulation (DNS) of solid-liquid flow.

Direct numerical simulation of solid-liquid flows is a way of solving the initial value problem for the motion of particles in fluids exactly, without approximation. The particles are moved by Newton's laws under the action of hydrodynamic forces computed from the numerical solution of the fluid equations. These equations are coupled through the no-slip condition on the particle boundaries, and through the hydrodynamic forces and torques that appear in the equations of rigid-body motion; they must be those arising from the computed motion of the fluid, and so are not known in advance, but only as the integration proceeds. It is crucial that no approximation of these forces and torques be made so that the overall simulation will yield a solution of the exact coupled initial value problem--yielding data as good as from experiments, but in a much more precise and usable form.

The application side of this project focuses on sand transport in fractured oil and gas reservoirs. This problem is representative of slurry transport in horizontal conduits where fluidization by lift is one of the main issues. We are trying to create engineering models which can be programmed on PCs and used to guide field practice.

We are able to solve problems with moderately high volume fractions, say even 50% solids when the particles are not too small, that is if the number of particles is not too large. Even in this case, the cost of computation is too great and the time of computation is too long. Moreover, we cannot yet simulate the motion of very small particles at the high volume fractions that we need to provide the optimal test for the models of slurry flow we wish to create.

1 Numerical methods

Direct numerical simulation (DNS) of solid-liquid flow. The current popularity of computational fluid dynamics is rooted in the perception that information implicit in the equations of fluid motion can be extracted without approximation using direct numerical simulation (DNS). A similar potential for solid-liquid flows, and multiphase flows generally, has yet to be fully exploited, even though such flows are of crucial importance in a large number of industries.

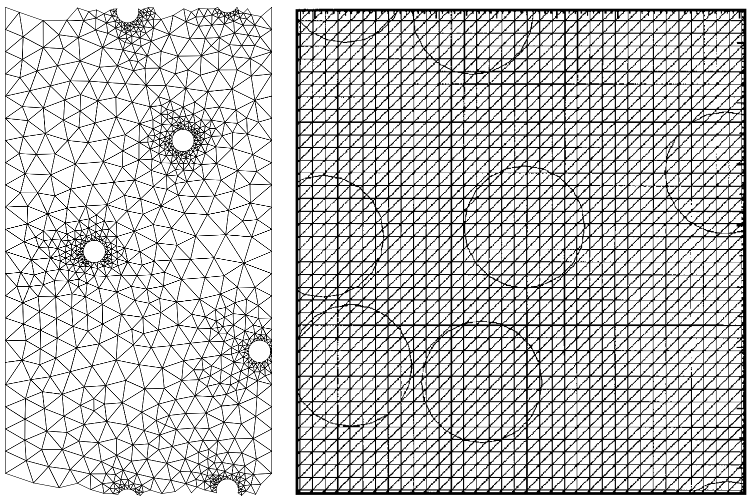

(a) (b)

Figure 1. ALE body-fitted, unstructured grid (a) compared with the fixed triangular grid (b) used in the DLM particle mover in which the bodies are filled with fluid and constrained to move as a rigid body by a distribution of Lagrange multipliers. The Lagrange multiplier fields and the associated variational rigid body constraint are analogous to the pressure field and the associated variational constraint of incompressibility. The DLM is as useful as it is elegant; fast solvers can be used and run matrix-free on the fixed grid and the problems of remeshing, projection and so on which plague methods based on unstructured grids, like ALE, have been circumvented. On the other hand, the DLM grids are not locally adaptive and they may not be as flexible for applications in irregular domains.

We have taken a major step toward the realization of this potential by developing two highly efficient parallel finite-element codes called *particle movers* for the direct numerical simulation of the motions of large numbers of solid particles in flows of Newtonian and viscoelastic fluids. One of the *particle movers* is based on moving unstructured meshes (arbitrary Lagranian-Eulerian or ALE) and the other on a structured mesh (distributed Lagrange Multiplier or DLM) using a new method involving a distribution of Lagrange multipliers to ensure that the regions of space occupied by solids are in a rigid motion (figure 1). Both methods use a new combined weak formulation in which the fluid and particle equations of motion are combined into a single weak equation of motion from which the hydrodynamic forces and torques on the particles have been eliminated. Several different kinds of code have been developed and tried on a variety of applications. See the project Web site, *http://aem.umn.edu/Solid-Liquid_Flows/*.

ALE Particle Mover. Direct simulation of the motion of solid particles in fluids can be said to have started in the paper of Hu, Joseph and Crochet 1992a. Three versions of the ALE code have emerged: Hu's [1996] integrated method in which the velocity and pressure are obtained at the same time; Choi's [2000] splitting method in which one solves sequentially for velocity and pressure; and Knepley's [1998] discretely solenoidal parallel code.

The ALE particle mover uses a generalization of the standard Galerkin finite-element method on an unstructured body-fitted mesh, together with an Arbitrary Lagrangian-Eulerian (ALE) moving mesh technique to deal with the movement of particles (see, for example Hansbo 1992, Huerta and Liu 1988, Nomura and Hughes 1992). In our implementation, the nodes on a particle surface are assumed to move with the particle. The movement of the nodes in the interior of the fluid is computed using a modified Laplace's equation, to ensure that they are smoothly distributed. At each time step, the grid is updated according to the motion of the particles. A new grid is generated whenever the elements of the mesh get too distorted, and the flow fields are projected onto the new grid.

Operator-splitting ALE Particle Mover. H. Choi 1999 developed a new solver for the ALE particle mover in the case of Newtonian fluids. The solver is based on a splitting method in which the divergence free condition is decoupled and generates a symmetric saddle point matrix and leads to a symmetric positive definite pressure equation. The pressure gradient is solved by a conjugate gradient method without preconditioning because the matrices involved are a composition of diagonally dominant matrices and other matrices conveniently formed with diagonal preconditioners. The methods run matrix-free of assembly of a global matrix. To have a well conditioned problem small time steps are usually required.

A Projected Particle Mover. Matt Knepley developed a variation of the ALE particle mover, Knepley, Sarin, Sameh 1998, in which the entire simulation is performed matrix-free in the space constrained to be discretely incompressible. Apart from the elegance of this approach, it simplifies the model by treating the particles and fluid in a decoupled fashion, and by eliminating pressure. The parallel multilevel preconditioner due to Sarin and Sameh 1998a, is used to obtain an explicit basis, P_v, for the discrete constrained divergence-free space. After elimination of pressure unknowns, a Krylov subspace method such as GMRES is used to solve the reduced system $P_v^T \tilde{A} P_v x = b$, where $\tilde{A}$ is the constrained Jacobian for velocity unknowns. In contrast to the ALE particle mover discussed earlier, the linear systems in this method are positive-definite, and exhibit favorable convergence properties on account of the well conditioned basis P_v. The algorithm has demonstrated very good scalability and efficiency for particle benchmarks on the SGI Origin 2000.

DLM Particle Mover. The DLM particle mover uses a new Distributed-Lagrange-Multiplier-based fictitious-domain method. The basic idea is to imagine that fluid fills the space inside as well as outside the particle boundaries. The fluid-flow problem is then posed on a larger domain (the "fictitious domain"). This larger domain is simpler, allowing a simple regular mesh to be used. This in turn allows specialized fast solution techniques. The larger domain is also time-independent, so the same mesh can be used for the entire simulation, eliminating the need for repeated remeshing and projection (see figure III.2). This is a great advantage, since for three-dimensional particulate flow the automatic generation of unstructured body-fitted meshes in the region outside a large number of closely spaced particles is a difficult problem. In addition, the entire computation is performed matrix-free, resulting in significant savings.

The velocity on each particle boundary must be constrained to match the rigid-body motion of the particle. In fact, in order to obtain a combined weak formulation with the hydrodynamic forces and torques eliminated, the velocity *inside* the particle boundary must also be a rigid-body motion. This constraint is enforced using a distributed Lagrange multiplier, which represents the additional body force per unit volume needed to maintain the rigid-body motion inside the particle boundary, much like the pressure in incompressible fluid flow whose gradient is the force required to maintain the constraint of incompressibility.

The rigid motion constraint has been implemented in two ways leading to two codes, DLM1 and DLM2. The first implementation DLM1 [29] requires that the fluid at the places $P(t)$ occupied by the solid take on a rigid body velocity

$$\text{DLM1 [29]} \quad \mathbf{u}(\mathbf{x},t) = \mathbf{U} + \boldsymbol{\omega} \wedge \mathbf{r}, \quad \mathbf{x} \in P(t)$$

where $\mathbf{U}$ is the velocity of the mass center and $\boldsymbol{\omega} \wedge \mathbf{r}$ is the rotation around the mass center. The second implementation DLM2 [74] is stress-like, rigid motion on $P(t)$ is enforced by requiring that the rate of strain vanish there

$$\text{DLM2 [74]} \quad \mathbf{D}[\mathbf{u}] = 0, \quad x \in P(t)$$

where $\mathbf{D}[\mathbf{u}]$ is the symmetric part of $\nabla\mathbf{u}$.

Parallel Implementation. The DL particle mover uses an operator-splitting technique consisting of three steps. In the first step, a saddle-point problem is solved using an Uzawa/conjugate-gradient algorithm, preconditioned by the discrete analogue of the Laplacian operator with homogeneous Neumann boundary conditions on the pressure mesh; such an algorithm is described in Turek 1996. The second step requires the solution of a non-linear discrete advection-diffusion problem that is solved by the algorithm discussed in Glowinski 1984. The third step solves another saddle-point problem using an Uzawa/conjugate-gradient algorithm.

The DLM approach uses uniform grids for two and three-dimensional domains, and relies on matrix-free operations on the velocity and pressure unknowns in the domain. This simplifies the distribution of data on parallel architectures and ensures excellent load balance (see Pan, Sarin, Glowinski, Sameh and Périaux 1998). The basic computational kernels, vector operations such as additions and dot products and matrix-free matrix-vector products, yield excellent scalability on distributed shared memory computers such as the SGI Origin 2000.

The main challenge in parallelization is posed by the solution of the Laplacian for the pressure mesh that functions as a preconditioner for the Uzawa algorithm. Fast solvers based on cyclic reduction for elliptic problems on uniform grids are overkill since the solution is required only to modest accuracy. A multilevel parallel elliptic solver, Sarin and Sameh 1998b, has been incorporated into the DLM1 algorithm. This has yielded speedup of over 10 for the preconditioning step on a 16 processor Origin.

The parallel DLM1 particle mover has been used to simulate the expansion of a fluidized bed. Even though, at present, there is a serial component of the code, we have observed an overall speedup of 10 on 16 processors of the SGI Origin 2000.

Viscoelastic DLM2 Particle Mover. The particle mover DLM2 has been implemented [90] for the popular Oldroyd-B constitutive model, which can be written in the form

$$\rho\left(\frac{\partial \mathbf{u}}{\partial t} + \mathbf{u}\cdot\nabla\mathbf{u}\right) = -\nabla p + \nabla\cdot(2\mu\mathbf{D} + \mathbf{A}), \qquad \nabla\cdot\mathbf{u} = 0,$$

$$\lambda_1\left(\frac{\partial \mathbf{A}}{\partial t} + \mathbf{u}\cdot\nabla\mathbf{A} - \mathbf{A}\cdot\nabla\mathbf{u} - \nabla\mathbf{u}^T\cdot\mathbf{A}\right) + \mathbf{A} = \frac{\eta_E}{\lambda_1}$$

where $\mathbf{D}$ is the rate-of-strain tensor, $\mathbf{A} = \tau_E + (\eta/\lambda)\mathbf{1}$ is the configuration tensor, τ_E is the elastic stress, η is the elastic viscosity, and λ_1 is the relaxation time. These equations are to be solved subject to appropriate boundary conditions.

2 Previous literature

Previous literature on the fluidization by lift of slurries is a small part of the literature on general solid-liquid flow which has been thoroughly discussed in several recent reviews [64, 50, 38.a, 30.a]. This literature can be grouped into DNS studies [22, 24, 25, 26, 32, 35, 38, 39, 40, 41, 42, 44, 47, 59, 65, 29, 37, 38, 74, 89, 90], analytic studies of lift of single particles [9, 12, 13, 15, 16, 17, (or 62, 63, 80,) 79, 85, 86, 87, 94], mixture theories [53, 46, 97, 45, 28, 96, 23, 20, etc], particle tracking methods in which particle forces are modeled [64, 4, 92, 72, 73], and several heuristic models of viscous resuspension [60, 1, 75, 67, 2].

Many authors refer to numerical codes which are faithful to the equations governing the fluid but are approximate in the way the solids are moved or in other ways, as direct numerical simulations. Point particle approximations have been used for dilute suspensions, especially for turbulent flow, to advect particles following Newton's laws. In some cases the influence of the particle on the fluid flow is neglected; in other cases the force on the fluid from the particles is added to the Navier-Stokes equation. Although this approach is often referred to as "DNS," the forces on each particle are related to its motions by semi-empirical relations and the effects of the particles on the fluid, as well as the interparticle interactions, must be modeled. Without giving here a long list of such approximations we simply point the reader to the excellent discussions and rather complete set of references in the papers [18, 30, 61, 66, 91].

The Lattice Bolzmann method (LBM) is an unconventional computational approach that constructs simplified kinetic models for the motion of discrete fluid particles. The LBM gives rise to particulate flows that are close to those computed by DNS [3,58,76] because the forces on the particles are computed rather than modeled.

Special cases of DNS have been developed by severely restricting the allowed motions, by ignoring viscous effects using inviscid potential flow [57, 7], or by ignoring fluid inertia completely as in Stokesian dynamics [51, 10, 55]. The potential flow simulations lead to cross-stream alignments due to inertia but the microstructural arrangements due to wakes cannot be captured. Stokesian dynamics cannot capture inertial effects but appear to give good descriptions of the flow of colloids of many particles at low Reynolds numbers. Another approach to interacting particle-liquid systems [36] which is closer to DNS but approximates the forces on the particles has been used to simulate the motion of 65000 particles at a Reynolds number of 0.5.

The literature on general forms of DNS is limited to the ALE and DLM *particle movers* developed by our team (see section 9) and the stabilized space-time finite element method of Tezduyar *et al* [93] in which the time coordinate is also discretized using finite elements. Using this method Johnson and Tezduyar [47, 48, 49] have simulated sedimentation of 1001 spheres at a Reynolds number of ten but computational difficulties are encountered at higher Reynolds numbers.

The literature on single particle lift is vast but the analytic studies are confined to potential flows with concentrated vorticity (aerodynamic lift [57]), to perturbations of potential flow with small distributed vorticity [7] and to perturbation studies of various kinds at low Reynolds numbers. All of the formulas can and will be tested by DNS; we can see if and where they are valid. Expressions for lift in slurries can be tested by DNS when they are proposed.

3 Applications of DNS

There are many ways in which DNS enters into applications. Here we are interested in using DNS to create and validate models. It is essential to understand that there are two very different types of models of solid-liquid flows: (1) those in which solid-liquid interactions must be modeled; such models arise from averaging, in mixture theories and in tracking codes that use modeled rather than computed forces. (2) "Effective" fluid models in which particle-laden regions of the fluid are modeled as an effective fluid with an effective viscosity, density and possibly other effective fluid properties. In this type of model the difficult problem of modeling forces may be avoided.

DNS can be used to create a data structure for testing models of lift and for understanding the dynamics that lead to this data. DNS can be used to create empirical forms for the effective properties of fluidized slurries and, more important, to distinguish cases in which effective property two-fluid models will work from those in which it won't.

Applications of DNS other than modeling are of value in engineering practice. For example, DNS can be used to improve understanding the dynamics of particulate flow. This is made possible by detailed and accurate numerical solutions of the initial value problem through which the motions of fluid and particle may be seen, processed and understood. It can also be used to generate empirical calculations formerly obtainable only from experiments. It can be used to create time and ensemble averaged solids fractions, solid and liquid velocities and other averaged quantities that enter into averaged continuum and mixture equations.

4 Fluidization by drag

Fluidized beds and sedimenting suspensions are controlled by a competition between buoyant weight and *drag*. The fluid flow and the particle motion are primarily in the same direction. Forces on the particle perpendicular to the motion are of secondary importance. The cooperative effects of the other particles in a fluidized suspension can be explained as hindered settling controlled by an effective viscosity and effective density of the mixture, and by back flow that gives rise a big slip velocity. These effects are evident in the two examples to follow.

Fluidization of 1204 spheres. Pan, Sarin, Joseph, Glowinski and Bai 2000 [70] have carried out DLM simulations of 1204 balls in a slit bed whose dimensions exactly match a real experiment. The simulation is compared with a matched real experiment and they give rise to essentially the same results. This simulation is presently at the frontier of DNS; it is a 3D computation of 1204 spheres at Reynolds numbers based on the sphere diameter of the order of 10^3 and the agreement with experiment is excellent. The details of the computation [70] and animations of the computations are on our web page. The computation is only partially parallelized and it is too expensive; it takes nearly 64 hours of computation time on the Origin 2000 with 4 processors to compute one second of real time.

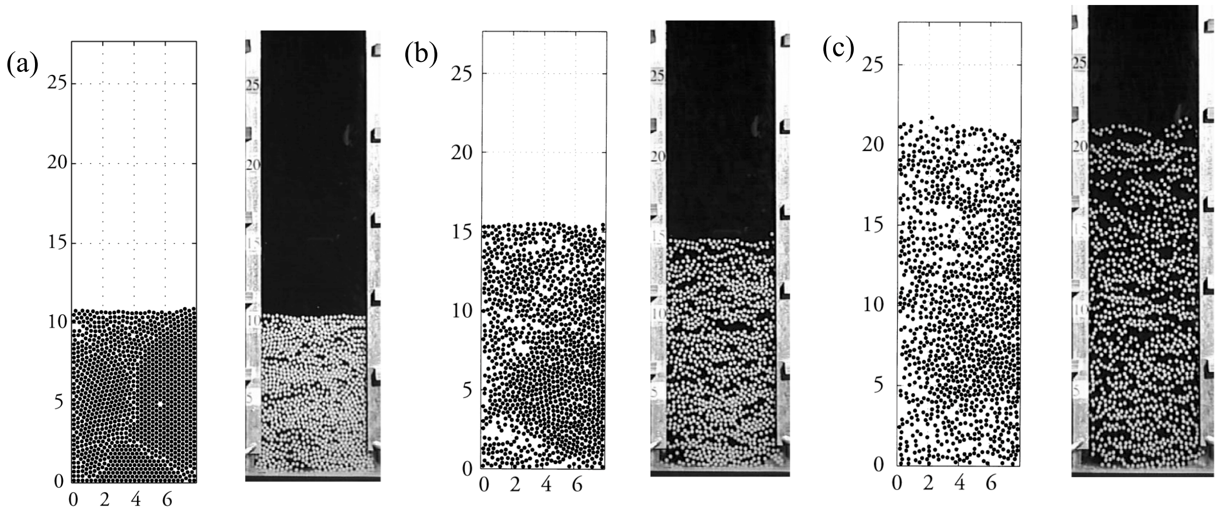

- V = 2 : Particle position at t = 5.625.
- The maximal particle Reynolds number is 1383.
- The maximal averaged particle Reynolds number is 130.

- V = 3.5 : Particle position at t = 17.238
- The maximal particle Reynolds number is 1671.
- The maximal avaraged particle Reynolds number is 236.

- V = 4.5 : Particle position at t = 31.
- The maximal particle Reynolds number is 1859.
- The maximal averaged particle Reynolds number is 292.

Figure 2. *Snapshots of fluidization of 1204 spheres comparing experiment (right) and simulation (left) (a)* V = *2, (b)* V = *3.5, (c)* V = *4.5.*

The computation shows that accurate direct simulation of real fluidized beds is possible and that the details of the particulate flow can be post processed and analyzed in ways not possible in real experiments. It shows that engineering correlations, here the Richardson-Zaki (RZ) correlation, can be obtained from data generated from DNS. The RZ correlation [70, 77] is given by

$$V(\phi) = V(0)\,(1-\phi)^n$$

where $V(\phi)$ is the composite velocity which is the volume flow rate divided by the cross-section area at the distributor when spheres of volume fraction p are fluidized by drag. $V(0)$ is the "blow out" velocity, when $\phi = 0$; when $V > V(0)$ all the particles are blown out of the bed. Clearly $V(\phi) < V(0)$. The RZ exponent $n(R)$ depends on the Reynolds number $R = V(0)d/\nu$, in a complicated but prescribed way.

The simulation of 1204 spheres was carried out in the bed [depth, width, height] = [0.686, 20.30, 70.22] cm. Snapshots comparing the animation with the experiment, in a frontal view are shown in figure 2. Figure 3 shows the rise curve vs. fluidizing velocity. Using all the data [70] we found from regression that

$$V(\phi) = V(0)\varepsilon^{n(R)} = 8.28^{2.33} \text{ cm}$$

The literature RZ value is 2.39 compared with our 2.33.

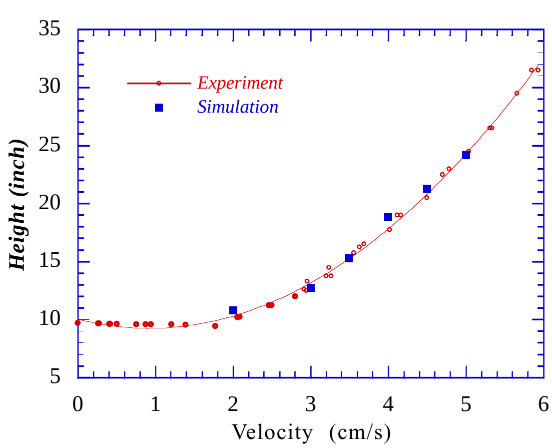

Figure 3. *Final bed height* H *vs. fluidizing velocity. The simulations give essentially the same height of rise as the experiments.*

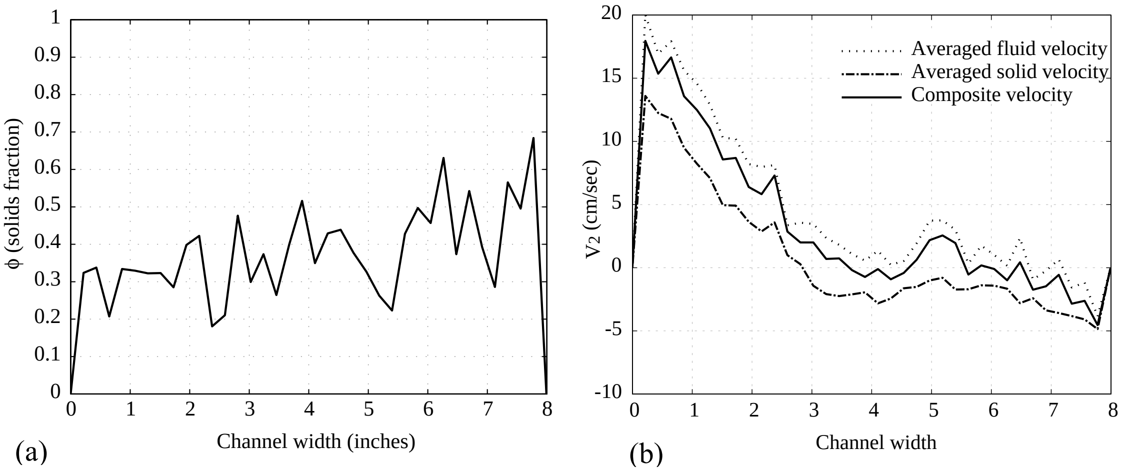

Figure 4. *Volume fraction* ϕ *and averaged components of velocity* V_2 *in coordinate direction* x_2 *at 38 nodes spaced at 1/10 in. across the 8 in. side of the fluidization column when* V = *4.5 cm/sec. (a)* ϕ*, (b)* V_2*. The difference between the averaged fluid and averaged solid velocity is the slip velocity. This is the first exact calculation of the slip velocity in a fluidized suspension.*

DLM produces huge amounts of data at each one of millions of nodes. The problem is how to structure this data to extract useful information; we must decide beforehand what data to collect as values to store for post processing. The fixed node property of DLM is particularly adapted to the collection of data in a form suitable for averaging methods used to construct models. To define a data structure we define a data string; this is a sequence of numbers produced at that node; one at each time step. Sometimes a particle is at the node, at other times the fluid is there. We can average the times the solid is there to get a solids volume fraction, if we average the velocity at the time steps of solid occupation, we get the average solids velocity. In the same way we can generate averages over the fluid. In figure 4 we display the distribution of solids fraction ϕ and the vertical velocity V_2 across the bed. The cross-stream velocities V_1 and V_2 actually average to zero as they should.

Sedimentation of 6400 circular particles [31]. Glowinski, Pan and Joseph 2000 presented a comparison of a numerical study using DLM by Glowinski and Pan of the sedimentation of 6400 circular particles with a two-fluid model of Joseph. This simulation gives rise to fingering which resembles Rayleigh-Taylor instability (see figure 5). The waves have a well-defined wavelength and growth rate which can be modeled as a conventional Rayleigh-Taylor instability of heavy fluid above light. The heavy fluid is modeled as a composite solid-liquid fluid with an effective composite density and viscosity. Surface tension cannot enter this problem and the characteristic short wave instability is regularized by the effective viscosity of the solid-liquid dispersion. The results of the simulation are in satisfying agreement with results predicted by the model without fitting parameters.

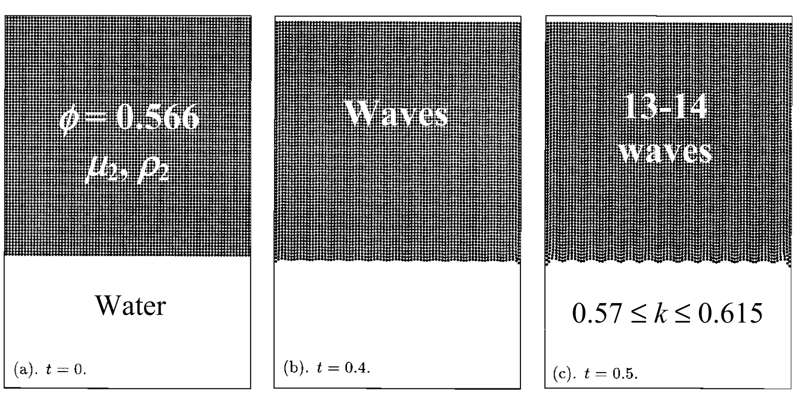

Figure 5. *Snapshots of the simulation of 6400 circles in 2D. The arrangement of sedimenting particles is asymetric, flat on top and corrugated at the bottom. The drag on a single sphere is smaller than when it is among many so that isolated spheres on the bottom fall out of the crystal and isolated spheres on the top fall into the crystal.*

The dispersion relation for Rayleigh-Taylor instability when surface tension is zero is given by

$$\rho_2 + \rho_f = \frac{k}{n^2}\left(\rho_2 - \rho_f\right)g - 2\frac{k^2}{n}\left(\eta_2 - \eta_f\right)$$

where ρ_f, η_f are the density and viscosity of water and ρ_2, η_2 are the effective density of the water-solid mixture. The disturbances are proportional to

$$e^{\text{int}} e^{1\left(k_x x + k_y y\right)} e^{\pm kz}, \; k = \sqrt{k_x^2 + k_y^2}$$

We modeled ρ_2 and η_2 with literature functions of the volume fraction, scaled for 2D.

$$\rho_2 = \rho_p \phi + \rho_f (1-\phi) = 0.1\phi + 1, \;\; \eta_2 = \eta_f \Big/ \left[1 - \frac{\phi}{0.833}\right]^2$$

The dispersion relation reduces to $2 = 55.4\ k/n^2 - 0.21k^2/n$. After maximizing n with respect we find that the maximum growth rate is $n = 12\ \text{sec}^{-1}$ for a wavelength $\lambda = 2\pi/k = 0.6$ cm. The values from direct simulation are $n = 13.4\ \text{sec}^{-1}$ and $0.57 \le k \le 0.615$ cm.

Several conclusions can be drawn from the calculation of the Rayleigh-Taylor instability of the two-fluid model of sedimentation of 6400 circles. The model does not require assumptions about the forces on the particles; it is an effective fluid model requiring an effective density and viscosity. The model is situation specific; we expect it to apply to Rayleigh-Taylor instability of sedimenting suspensions with different size circles, different densities, volume fractions, in 3D, etc. Our view is that one two-fluid will not work for all situations; the specification of the domain of applicability of a model is as important as the form of the model.

5 Fluidization by lift

Saltation and fluidization of particles in slurries flowing perpendicular to gravity are controlled by a competition between buoyant weight and *lift*. Forces on the particles perpendicular to the motion are of primary importance. The cooperative effects of the other particles in the slurry can possibly be explained by hindered motion rather than by hindered settling. Here the effective viscosity and density of particle-laden regions are important but back flow is negligible and the concept of slip flow has to be reinterpreted.

Sand transport in fractured reservoirs. The problem of transport of particles by fluids in horizontal conduits and pipes is of considerable scientific and industrial importance and is the focus of this paper. This problem arises in the transport of coal-water slurries, in the removal of drill cuttings in drilling of horizontal oil wells and in proppant transport in hydraulically fractured rock in oil and gas bearing reservoirs, to name a few. The central unsolved fluid dynamics problem arising in these applications is the problem of fluidization by lift. The problem of fluidization by lift can be well framed in the problem of hydraulic fracturing.

Hydraulic fracturing is a process often used to increase the productivity of a hydrocarbon well. A slurry of sand in a highly viscous, usually elastic, fluid is pumped into the well to be stimulated, at sufficient pressure to exceed the horizontal stresses in the rock at reservoir depth. This opens a vertical fracture, some hundreds of feet long, tens of feet high, and perhaps an inch in width, penetrating from the well bore far into the pay zone. When the pumping pressure is removed, the sand acts to prop the fracture open. Productivity is enhanced because the sand-filled fracture offers a higher-conductivity path for fluids to enter the well than through the bulk reservoir rock, and because the area of contact for flow out from the productive formation is increased. It follows that a successful stimulation job requires that there be a continuous sand-filled path from great distances in the reservoir to the well, and that the sand is placed within productive, rather than non-productive, formations.

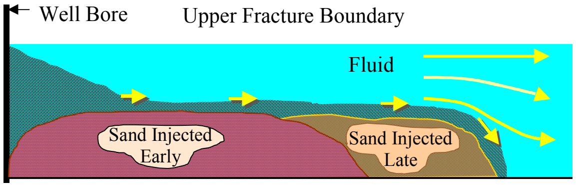

Figure 12. Sand transport in a fractured reservoir [55] is different than the eroded bed of 300 particles in figure 8(a) and 9(a) because particles are injected. The creation of algorithms to simulate continuous injection is one of our simulation projects.

In a slot problem a particle laden (say 20% solids) fluid is driven by a pressure gradient and the particles settle to the bottom as they are dragged forward. Sand deposits on the bottom of the slot; a mound of sand develops and grows until the gap between the top of the slot and the mound of sand reaches an equilibrium value; this value is associated with a critical velocity. The velocity in the gap between the mound and the top of the slot increases as the gap above the mound decreases. For velocities below critical the mound gets higher and spreads laterally; for larger velocities sand will be washed out until the equilibrium height and velocity are reestablished (see figure 12). The physical processes mentioned here are *settling* and *washout*. Washout could be by sliding and slipping; however, a more efficient transport mechanism is by *advection after suspension* which we studied by direct simulation.

The fracturing industry makes extensive use of models and correlations programmed for PCs to guide field operations. These models are developed to predict how the fracture crack opens and closes and how proppant is transported in the crack. Commercial packages dealing with these problems and proprietary packages developed by oil service companies are used extensively. None of these packages model the all-important levitation of proppants by hydrodynamic lift.

Controlling parameters. Problems of fluidization by lift in a shear flow driven by a pressure gradient can be separated into (1) single particle studies [71] in which the factors that govern lifting of a heavier-than-liquid particle off a wall by a shear flow are identified and (2) many (300) particle studies [14] in which cooperative effects on lift-off and hindered motions are important. The computations [71, 14] were ALE, 2D simulations of the lifting of circular particle; we can and will do DLM simulations of spheres in 3D next.

Important information about particulate flow of spheres in plane Poiseuille flow can be obtained from a dimensionless form of the governing equations, div **u** = 0, the Navier equations for an incompressible fluid and Newton's equations for the acceleration of the mass center and torque on a rigid body. The equations are made dimensionless with scales [d, v, d/v, $\eta\ V/d$] = [length, velocity, time, stress and pressure] and the resulting dimensionless equations are completely determined when the ratios d/W (W is the channel height) and ρ_p/ρ_f and the shear Reynolds number (R) and gravity parameter (G) are given, where

$$R = \frac{\rho_f V d}{\eta} = \frac{\rho_f W d^2 \overline{p}}{\eta} = \frac{\rho_f \gamma_w d^2}{\eta}, \tag{1}$$

$$G = \frac{(\rho_p - \rho_f) g d^2}{\eta V} = \frac{2(\rho_p - \rho_f) g d}{W \overline{p}} = \frac{(\rho_p - \rho_f) g d}{\eta \gamma_w}. \tag{2}$$

The pressure gradient $\overline{p}$ is related to the wall shear rate $\dot{\gamma}_w$ by $\overline{p} = 2\eta\dot{\gamma}_w / W$. For given density and aspect ratios, particulate Poiseuille flow of one single particle is completely determined by the values of the shear and gravity Reynolds numbers. The dynamics of many particles of course depends also on the distribution and motions of the other particles; the simplest approach to these other particle effects is a hindered motion function of the solids fraction ϕ.

Instead of R and G, we may look to the product and ratio.

$$R_G = RG = \frac{(\rho_p - \rho_f)\rho_f g d^3}{\eta^2} = \frac{\left(\frac{\rho_p}{\rho_f} - 1\right) g d^3}{\nu^2}, \quad \text{(Reynolds number based on sedimentation velocity)} \tag{3}$$

$$\frac{R}{G} = \frac{\gamma_w^2 d}{\left(\frac{\rho_p}{\rho_f} - 1\right) g} = \frac{\left(\gamma_w d^2\right)^2}{\left(\frac{\rho_p}{\rho_f} - 1\right) g d^3} \quad \text{(Generalized Froude number)} \tag{4}$$

The first of these ratios represents the ratio of buoyant weight to viscous resistance; settling is rapid when this number is large. The second number represents the ratio of inertial lift due to shear to the buoyant weight.

Single particle lift off and levitation to equilibrium. The problem of lift off and levitation to equilibrium of a single circular particle in a plane Poiseuille flow was simulated using an ALE particle mover in [71]. The principal features of lift off and levitation to equilibrium are listed in the caption of figure 6. Heavier particles are harder to lift off. The critical lift off Reynolds number increases strongly with the density ratio (see table 1). The height, velocity and angular velocity of the particle at equilibrium is given as a function of prescribed parameters in tables and trajectories from lift-off to equilibrium in graphs shown in [71].

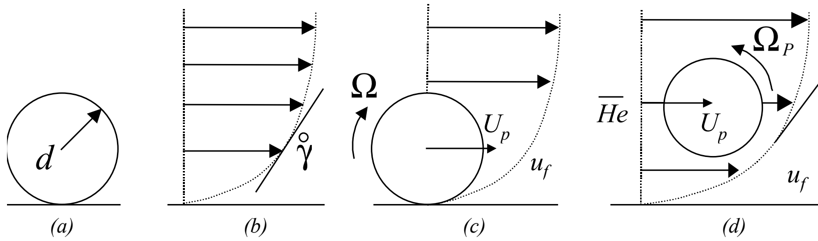

Figure 6. Lift off and levitation to equilibrium. The pressure gradient in the flow and on the particle is increased. The heavier than liquid particle slides and rolls on the bottom of the channel. At a critical speed the particle lifts off. It rises to a height in which the lift balances the buoyant weight. It moves forward without acceleration at a steady velocity and angular velocity.

The data on steady flow that is generated by DNS can be used to improve understanding and to create and validate correlations and models. In [71] well known expressions of Bretherton (1992) for the lift

$$L = \frac{21.16\eta U_s}{\left(0.679 - \ln\left(\sqrt{R/4}\right)\right)^2 + 0.634} \tag{5}$$

and drag

$$D = \frac{4\pi\eta U_s \left(0.91 - \ln\left(\sqrt{R/4}\right)\right)}{\left(0.679 - \ln\left(\sqrt{R/4}\right)\right)^2 + 0.634} \tag{6}$$

at low Reynolds numbers $R = \rho_f \dot{\gamma}_w d^2 / \eta$ were tested by DNS; the lift and drag were computed for prescribed values of the slip velocity U_s. The results are presented in table 2. The only way to test formulas for lift and drag in 2D, which cannot be realized in experiments, is by DNS. In natural cases in which no engine moves the particle forward, the acceleration of the particle vanishes when the lift balances the buoyant weight; this condition applies to (5) would give a definite value for U_s. There are many formulas for the lift, drag, equilibrium height, velocity and angular velocity at low R in 3D; we propose to test all those formulas with DNS.

Table 1. Critical Reynolds numbers for lift off at different values of RG.

ρ_s / ρ_f	1.001	1.01	1.4
Critical R	0.33	2.83	25

		$\rho_f U_s d/\eta$ = 0.003			$\rho_f U_s d/\eta$ = 0.1		
		DNS	Analytic	% Error	DNS	Analytic	% Error
***R* = 0.01**	Lift	0.00347	0.00449	-22.72	0.08593	0.1496	-42.56
	Drag	0.01010	0.01041	-2.98	0.3374	0.3471	-2.79
***R* = 0.02**	Lift	0.00436	0.00542	-19.56	0.1239	0.1806	-31.39
	Drag	0.01093	0.01145	-4.54	0.3637	0.3818	-4.74

Table 2. Comparison between the numerical and analytic values of lift and drag per unit length in CGS units. Error is calculated with respect to the analytic value.

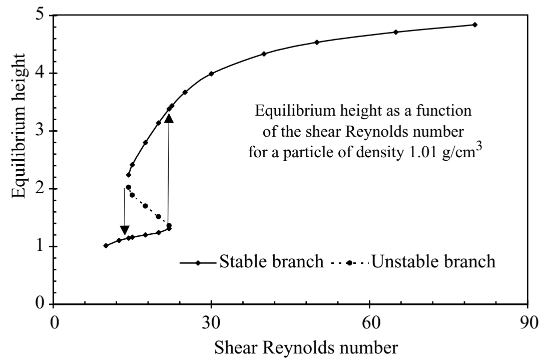

Figure 7. Turning point "bifurcations" shown in the height vs. Reynolds number curve. There are two stable branches separated by an unstable branch.

DNS results given in [71] show that a circular particle will rise higher when the rotation of the particle is suppressed and least when the slip angular velocity is put to zero; the freely rotating zero torque case lies between. DNS allows such a comparison, which would be difficult or impossible to carry out in an experiment.

A turning point bifurcation of steady forward flow of a single particle at equilibrium was found in direct simulations of rise trajectories reported in [14]; the height and particle velocity change strongly at such a point. A computational method advanced in [71] looks for the points on lift vs. height curve at which lift balances buoyant weight. This gives both stable and unstable solutions and leads to the "bifurcation" diagram shown in figure 7, which shows there are two turning points, hysteresis, but no new branch points. Such an instability was previously unknown; we propose to verify the similar turning point bifurcations that appear in simulations of lifting of spheres in 3D.

Levitation to equilibrium of 300 circular particles. The transport of a slurry of 300 heavier than liquid particles in a plane pressure driven flow was studied using DNS in [14]. Time histories of fluidization of the particles for three viscous fluids with viscosities η = 1, 0.2 and 0.01 (water) were computed at different pressure gradients. The study leads to the concept of fluidization by lift in which all the particles are suspended by lift forces against gravity perpendicular to the flow.

The time history of the rise of the mean height of particles at a given pressure gradient is monitored and the rise eventually levels off when the bed is fully inflated. The time taken for full inflation decreases as the pressure gradient (or shear Reynolds number) increases (see figure 8). The bed does not inflate when the critical value is below the critical value for lift off of a single particle.

At early times, particles are wedged out of the top layer by high pressure at the front and low pressure at the back of the particle in the top row (t = 1 in figure 8a, t = 0.9 in figure 8b).

The dynamic pressure at early times basically balances the weight of the particles in the rows defining the initial cubic array. This vertical stratification evolves into a horizontally stratified propagating wave of pressure, which tracks waves of volume fraction. The pressure wave is strongly involved in the lifting of particles. For low viscosity fluids like water where *RG* is large the particle-laden region supports an "interfacial" wave corresponding to the wave of pressure. If *R/G* is large the interface collapses since the stronger lift forces push wave crests into the top of the channel, but the pressure waves persist (figure 9).

A simple analytic model for the free motion of a single long particle of diameter d in Poiseuille gives rise to a formula for the particle velocity

$$U_p = \left(\frac{W+d}{W-d}\right)\left(1-\frac{y_1-d/2}{y_1}\right)\left(1-\frac{W-y_1-d/2}{W-y_1}\right)U(y_1)$$

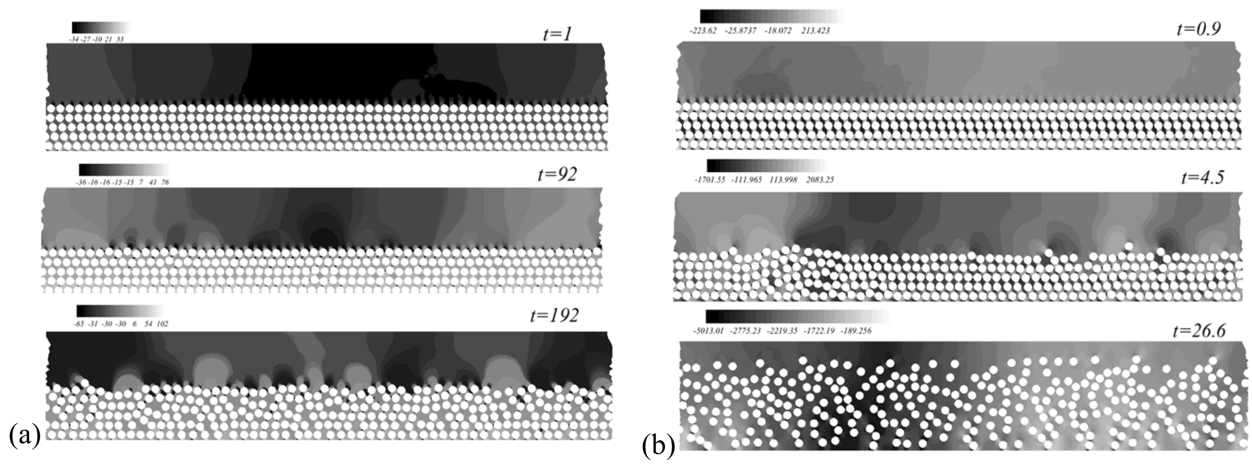

*Figure 8. (a) Snapshots of the fluidization of lift of 300 circular particles ρ_p = 1.01 g/cm^3 when η = 1 poise (*R = *5.4,* G *= 1.82). The flow is from left to right. The gray scale gives the pressure intensity and dark is for low pressure. At early times particles are wedged out of the top layer by high pressure at the front and low pressure at the back of each and every circle in the top row. The vertical stratification of pressure at early times develops into a "periodic" horizontal stratification, a propagating pressure wave. The final inflated bed has eroded, rather tightly packed at the bottom with fluidized particles at the top. (b) Fluidization of 300 particles (*R *= 120,* G *= 0.08). The conditions are the same as in 8(a) but the ratio of lift to buoyant weight is greater and the fluidization is faster and the particle mass center rises higher than in the previous figures.*

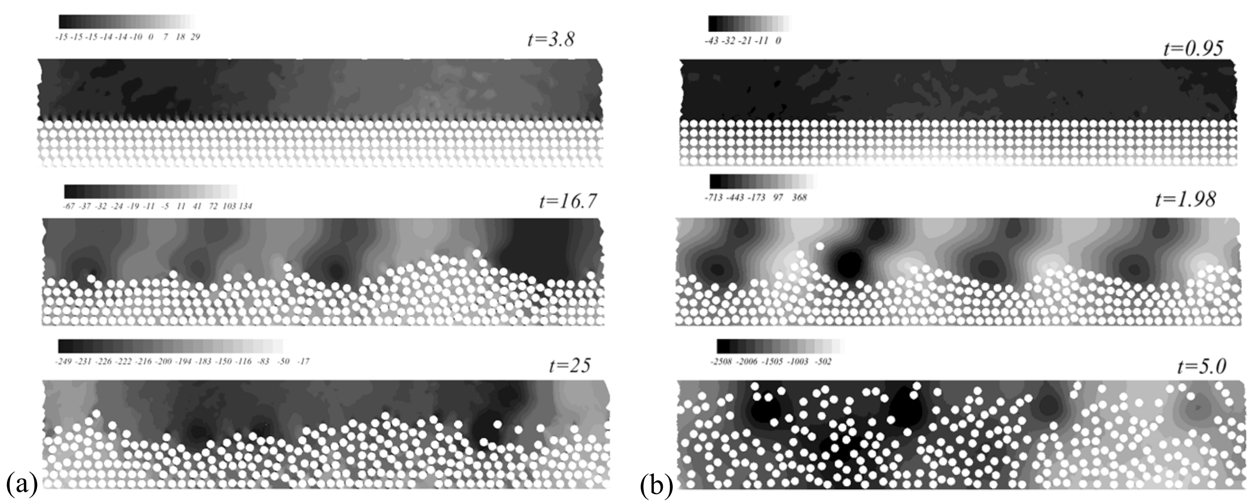

Figure 9. (a) Fluidization of 300 particles (η = 0.2 poise, R *= 150,* G *= 1.63). The final state of the fluidization at* t *= 25 sec has not fully eroded. The particles that lift out of the bed can be described as saltating. A propagating "interfacial" wave is associated with the propagating pressure wave at* t *= 25. (b). Fluidization of 300 particles (η = 0.2 poise,* R *= 450,* G *=0.54). The flow is from left to right. The particles can be lifted to the top of the channel.*

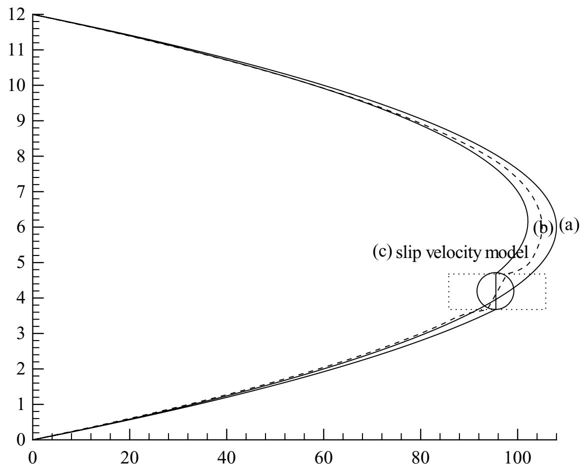

Figure 10. Velocity profiles for three different solutions with W = 12 cm, d = 1 cm, η = 0.2 poise and $\overline{p}$ = 1.2 dynes/cm^3. (a) Undisturbed Poiseuille flow (b) DNS of one circular particle lift h_e = 4.18 cm (see Table 1) (c) model problem with y = 4.18 cm. The model reduces the velocity more because the particle is long and does not rotate.

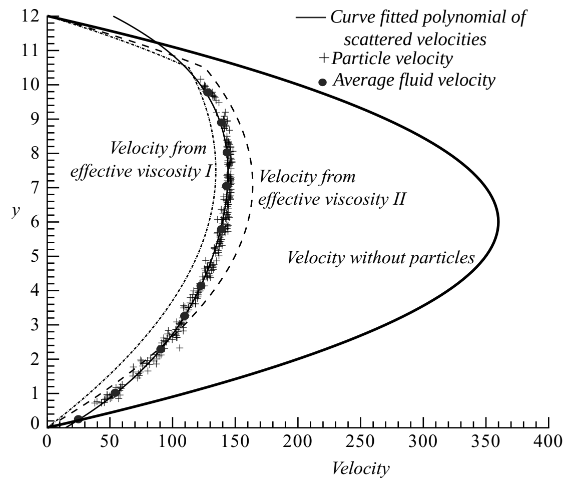

Figure 11. Comparison of the average velocity profile in the slurry of 300 particles with the Poiseuille profile in the pure fluid (η = 1 poise). The particles "hold up" the fluid. The increased drag on the fluid due to the free particles can be modeled as an effect of an effectively increased viscosity of the fluid-solid mixture.

where y_1 is the distance from the channel bottom to the particle center, $U(y_1)$ is fluid velocity at y_1 when no particle is present and W is the channel height. The slip velocity $U(y_1) - U_p > 0$ is positive but tends to zero with the particle diameter. The presence of particles produces a lag in the fluid velocity and the effect of such a drag can be interpreted as an effectively increased viscosity for the fluid-solid mixture. The effect of one particle of finite size on the undisturbed flow is global (figure 10).

DNS data can be sampled for average fluid and average solid velocities. Such a sampling is shown in figure 11. The difference between these velocities is very small, but the difference between the composite velocity and the particle free Poiseuille is dramatic.

We attempted to model the average flow of the slurry by a two-fluid model in which the particle-laden region is treated as a fluid with an effective viscosity; for this calculation we used two different well regarded formulas for the effective viscosity, with pure liquid above the mean height and effective liquid below. We would like to be able to predict the mean height from considerations involving also an effective density.

6 Future work

Our program of research focuses on (1) developing DLM *particle movers* which run on many processors, (2) developing procedures for intelligent interrogation of DNS, (3) modeling studies of lift based on DNS and (4) modeling studies of proppant transport in fractured reservoirs.

Parallel preconditioners for DLM. One of the goals of this project is to further accelerate the convergence of the solvers by using clever preconditioning techniques. We have a number of promising approaches to investigate. The projected ALE particle mover we have developed uses the highly effective multilevel approach to restrict the Navier-Stokes systems to a discretely divergence-free space. This results in well-conditioned systems for small time steps that can be solved in parallel with high efficiency. For large time steps, however, we need powerful preconditioning of the reduced system itself. The matrix-free multilevel approach for constructing discretely divergence-free spaces has been highly successful for the generalized Stokes problem. Exploiting similarities of the reduced system with the stream-vorticity formulations, we have been successful in designing preconditioners.

Formulate calculation procedures that allow for continuous injection of particles into the computational cell. Our particle movers can handle cases in the number of particles in a cell are fixed; the cell is either stationary and spatially periodic or is a moving cell of finite length which moves with the particles. In fracturing applications sand is continuously injected as shown in figure 12.

Collision Strategies. It is not possible to simulate the motion of even a moderately dense suspension of particle without a strategy to handle cases in which particles touch. In unstructured-grid methods, frequent near-collisions force large numbers of mesh points into the narrow gap between close particles and the mesh distorts rapidly, requiring an expensive high frequency of remeshing and projection. A "collision strategy" is a method for preventing near collisions while still conserving mass and momentum.

Four collision strategies are presently being used [37, 29, 61a, 47]. They all define a security zone around particle such that when the gap between particles is smaller than the security zone a repelling force is activated. The repelling force pushes the particle out of the security zone into the region in which fluid forces computed numerically govern. The strategies differ in the nature of the repelling force and how it is computed. All of these strategies keep the particles farther apart than they ought to be, resulting in too high void fractions.

To have real collision of smooth rigid particles it is necessary for the film between particles to rupture and film rupture requires physics and mathematics beyond the Navier-Stokes equations. A goal for future simulations is to develop particle movers that make no special provision collisions or contact, relying on the equations of motion to prevent them. This goal can possibly be achieved within limits set by the mesh size by placing the security zone inside the particle, in a small layer, and allowing the particles to overlap in dynamic simulation. This would allow the natural hydrodynamics to act within mesh tolerance in dynamics. Overlap in statics could not occur because a repelling force would be activated to push them apart and close packed static arrays would then develop.

Interrogation of DNS. In previous studies of lift of single circular particles in 2D [71] we generated rise trajectories and created tables of the final height of rise, the velocity and angular velocity of the particles at the final height of rise and the bifurcation of scenarios for different values of the shear Reynolds number, gravity, viscoelastic and other parameters. Similar tables for average values in fully inflated beds of 300 particles were created [14]. These quantities define a data structure generated by DNS, which can help in the creation and validation of lift models; the tables give the answers to which models aspire.

Modeling studies for lift based on DNS. The simulated results are like experiments and give rise to "experimental" results but in a more detailed form in which separate effects can be examined at low cost.

We are going to do 3D simulations of fluidization by lift for single spheres, many spheres and very many heavy spheres, in that order. We are going to fluidize these spheres in plane shear flows and in pressure gradient driven channel flows and in rectangular conduits where the effects of side walls can be important.

Our DLM particle mover does not need to be enhanced to carry out 3D simulations for channel flows. We propose to generate rise to equilibrium curves and the value of the equilibrium height, particle velocity and angular velocity, slip velocity and slip angular velocity for non-accelerating neutrally buoyant and heavier-than-liquid single spheres. The simulations allow us to vary the conditions under way; we can prescribe the angular velocity and compute the torque or prescribe the forward velocity and compute the drag, as we have done in 2D.

Validation of lift formulas for single spheres. There are a small number of explicit formulas for lift and many more for drag on a single sphere in shear flows. These formulas are derived in distinguished limits, like low Reynolds number, in which the effects of inertia or non-Newtonian effects can be obtained as perturbations of linearized low Reynolds number equations (a list of papers giving such formulas are listed under prior literature). The formulas make explicit the dependence of lift and drag on the properties of the fluid and solid and the flow, but the limits of validity of these have not been established. For example it is not known how fast formulas said to be valid at low Reynolds will lose validity as the Reynolds number is increased. It is very hard to validate these formulas and their dependence on parameters with experiments; basically the formulas have not been verified by experiments.

Every formula for lift and drag on single spheres can be examined for accuracy by DNS. For the problem of fluidization of lift the free particle studies leading to data sets previously mentioned are of interest. Using DNS, we can completely clarify if, when, where the analytic formulas are valid and useful. An example is the test we made of Bretherton's 2D formulas (5) and (6) leading to table 2.

Generation of lift and drag formulas at finite Reynolds numbers. At finite Reynolds numbers, the only formulas for drag are empirical and there are no formulas for lift of single spheres in the presence of a plane wall or when wall effects are neglected. We may generate the values of lift and drag for single spheres at finite Reynolds numbers under all conditions. We have the data to construct empirical (simulated) formulas under conditions in which analysis is impossible and experiments are difficult, expensive and in any case give rise to mixed data in which the factors that determine cannot be treated separately.

Compute the bifurcations of equilibrium solutions for the lifting of single spheres in shear flow under different conditions. Our 2D DNS calculations revealed that the double turning point bifurcations (figure 7) of the rise to equilibrium solutions for circular particles in shear flows are a generic phenomenon; they occur for different weights and sizes and when the particle is free or rotation is suppressed.

We are proposing to establish the bifurcations of equilibrium solutions for single spheres in 3D shear flows, examining the effects of nearby side walls on the rise of spheres in rectangular conduits.

Effective property models. Hindered settling is a topic which arises in problems of fluidization by drag, in fluidized beds and sedimenting suspensions where lift forces are not important. Slip velocities are important in these problems but our 2D simulations show that slip velocities defined as the difference of the average fluid and solid velocities are very small in suspensions fluidized by lift. What we have in these flows is a hindered forward motion rather than hindered settling.

The simulations of 300 circles show that particle-laden regions can be dearly demarcated from clear fluid regions, see figures 8-11. This suggests that motion may be represented as by two fluids, clear fluid and an effective fluid representing the fluid-solids mixture. The animations and the analysis of DLM data suggest the particle-laden flow may be partitioned into several, even one region, with uniform solid fraction. We would like to use the DNS, particularly volume fraction data, which could be used to create effective fluid models based on the calculation of effective viscosity and effective density for the mixture.

Proppant (sand) transport. This problem is a general surrogate for the problem of modeling slurry transport of very many small heavy particles in rectangular channels (fractured reservoirs) under the condition of continuous injection We cannot yet generate a DNS database for this problem. Innovative approaches for new solvers and preconditioners which scale well onto many processors are required as are the procedures which would allow us to treat problems in which there is a net increase or decrease of particles in the computational domain.

It is possible to carry out studies of proppant of many particles, if not very many small and heavy particles, in periodic or moving domain rectangular cells not different than those described earlier.

Wall effects on proppant transport. Huang and Joseph [43] studied the migration of 56 particles in plane Poiseuille flow. This was a two dimensional computation in which the separate and combined effects of shear thinning and elasticity were investigated. Shear thinning drives the fluid away from the center but they stay away from the wall; elasticity drives the particles to the channel center. When shear thinning is combined with elasticity some particles migrate strongly to the wall and the others group at the center, leaving a clear annulus of fluid between. A great advantage of DNS is that you can turn physics on and off which is something that can't be done in nature.

Effects of normal stresses and shear thinning on the transport of proppants in viscoelastic fluid. These effects can be dramatic in cross linked fluids often used to carry proppants into fractures. We are able to do these simulations, but with a smaller number of particles than in Newtonian fluids. As in the Newtonian case, we plan to do 2D studies with large numbers O(10K) of small particles to better represent conditions that prevail in actual reservoirs. Wall effects in the viscoelastic are different and they will also be studied in 3D simulations of slot flow using the new viscoelastic DLM particle mover developed by P. Singh. As a practical matter for applications we need to identify a few fluid parameters besides viscosity that describe the gross behavior of non-Newtonian fracturing fluids. The fluid parameters we presently favor are the shear thinning index and fluid relaxation time.

Useful correlations for hydrodynamic lifting of slurries of proppants. We have had some initial success at processing DNS relating lift on a single circular particle with the lift on a particle in a slurry of solids fraction ϕ. This kind of correlating follows along lines of the Richardson-Zaki correlations [77] for slurries fluidized by drag. We are going to use data from DNS in 3D to create correlations and these correlations validated by DNS are also to be compared with real experiments.

Dimensionless parameters. It is surprising that the list of dimensionless parameters that control solid-liquid flow is unknown to modelers in the fracturing and appear not to have been so clearly set out in academic studies. The two Reynolds numbers (1) and (3) are especially important.

References

1 R.R. Abbot, N. Tetlow, A.L. Graham, S.A. Altobelli, E. Fukushima, L.A. Mondy and T.S. Stevens. Experimental observations of particle migration in concentrated suspensions: Couette flow, *J. Rheol*. **35**, 773-795 (1991).

2 A. Acrivos. Shear-induced particle diffusion in concentrated suspensions of noncolloidal particles, *J. Rheol*. **39**, 813-826 (1995).

3 C.K. Aidun, Y. Lu and E. Ding. Direct analysis of particulate suspensions with inertia using the discrete Boltzmann equation, *J. Fluid Mech.* **373**, 287, (1998).

4 M.J. Andrews and P.J. O'Rourke. The multiphase particle-in-cell (MP-PIC) method for dense particulate flows, *Int. J. Multiphase Flow* **22**, 379-402 (1996).

5 E.S. Asmolov. Dynamics of s spherical particle in a laminar boundary layer, *Fluid Dyn*. **25**, 886-890 (1990).

6 E.S. Asmolov. The inertial lift on a spherical particle in a plane Poiseuille flow at large channel Reynolds number, *J. Fluid Mech.* **381**, 63-87 (1999).

7 T.R. Auton. The lift force on a spherical body in a rotational flow, *J. Fluid Mech.* **183**, 199-218 (1987).

8 R. Bank, B. Welfert, and H. Yserentant. A class of iterative methods for solving saddle point problems. *Numer. Math.,* **56**:645-666 (1990).

9 T. B. Benjamin. Note on formulas for the drag of a sphere, *J. Fluid Mech.*, **246**, 335 (1993).

10 J. F. Brady. Stokesian Dynamics simulation of particulate flows, in Particulate Two-Phase Flow, (M.C. Roco, ed.), 971-998, (1993), Butterworth - Heinemann.

11 J. F. Brady & G. Bossis. Stokesian dynamics, *Ann. Rev. Fluid Mech.* **20**, 111-157 (1988).

12 F.P. Bretherton. Slow viscous motion round a cylinder in simple shear, *J. Fluid Mech*. **12**, 591, (1962).

13 P. Cherukat and J. McLaughlin. The inertial lift on a rigid sphere in a linear shear flow field near a flat wall, *J. Fluid Mech.* **263**, 1–18 (1994).

14 H.H. Choi and D.D. Joseph. Fluidization by lift of 300 circular particle in plane Poiseuille flow by direct numerical simulation. To appear (see : *http://www.aem.umn.edu/Solid-Liquid_Flows*) (2000).

15 R.G. Cox and S.K. Hsu. The lateral migration of solid particles in a laminar flow near a plane. *Intl. J. Multiphase Flow*, **3**, 201 (1977).

16 R.G. Cox and S.G. Mason. Suspended particles in fluid flow through tubes, *Ann. Rev. Fluid Mech.* **3**, 291, (1971).

17 R.G. Cox, I.Y. Zia and S.G. Mason. Particle motions in sheared suspensions. XXV. Streamlines around cylinders and spheres, *J. Colloid Interface Sci.* **27**, 7 (1968).

18 E. Dean, R. Glowinski, and T.-W. Pan, A Wave Equation Approach to the Numerical Simulation of Incompressible Viscous Fluid Flow Modeled by the Navier-Stokes Equations, in *Proceedings of the SIAM/INREA Wave Progagation Conference* To appear.

19 W. D'orfler. The conditioning of the stiffness matrix for certain elements approximating the incompressibility condition in fluid dynamics. *Numer. Math.,* **58**:203-214 (1990).

20 D.A. Drew & S.L. Passman. Theory of Multicomponent Fluids, Springer-Verlag, New York (1999).

21 N. Dyn and J. W.E. Ferguson. The numerical solution of equality-constrained quadratic programming problems. *Math. Comp.,* **41**(163):165-170 (1983).

22 H. Elman and D. Silvester. Fast Nonsymmetric Iterations and Preconditioning for Navier-Stokes Equations, *CS-TR* 3283 and *UIACS-TR* 94–66, University of Maryland (1994).

23 L.S. Fan, & C. Zhu. Principles of Gas-Solid Flows, Cambridge Univ. Press (1998).

24 J. Feng, H. H. Hu, and D. D. Joseph. Direct Simulation of Initial Value Problems for the Motion of Solid Bodies in a Newtonian Fluid. Part 1: Sedimentation, *J. Fluid Mech.* **261**, 95–134 (1994).

25 J. Feng, D. D. Joseph, and P. Y. Huang. The Motion and Interaction of Solid Particles in Viscoelastic Liquids, *Rheol. Fl. Mech. Nonlin. Mat*. **217**, 123–133 (1996).

26 A. Fortes, D. D. Joseph, and T. S. Lundgren. Nonlinear Mechanics of Fluidization of Beds of Spherical Particles, *J. Fluid Mech.* **177**, 467–483 (1987).

27 M. Fortin and R. Glowinski. *Augmented Lagrangian Methods: Applications to the Numerical Solution of Boundary-Value Problems*. North-Holland, New York (1983).

28 D. Gidaspow. Multiphase Flow and Fluidization Continuum and Kinetic Theory Description. Academic Press, Boston, MA (1994).

29 R. Glowinski, T.-W. Pan, T.I. Hesla, and D.D. Joseph. A Distributed Lagrange Multiplier/Fictitious Domain Method for Flows Around Moving Rigid Bodies: Application to Particulate Flows, *Int. J. Multiphase Flow* **25**, 755-794 (1999).

30 R. Glowinski, T.-W. Pan, T.I. Hesla, D.D. Joseph, and J. P´eriaux, A Fictitious Domain Method with Distributed Lagrange Multipliers for Numerical Simulation of Particulate Flows, in *Proceedings of the Tenth International Conference on Domain Decomposition Methods*, Boulder, Colorado (1997).

30.a R. Glowinski, T.-W. Pan, T.I. Hesla, D.D. Joseph, and J. P´eriaux, A Fictitious Domain Approach to the Direct Numerical Simulation of Incompressible Viscous Flow Past Moving Rigid Bodies: Application to Particulate Flow, to appear in *J. of Computational Physics*, (2000).

31 R. Glowinski, T.W. Pan and D.D. Joseph. Modeling Rayleigh-Taylor Instability of a Sedimenting Suspension Arising in Direct Numerical Simulation, to appear (see : *http://www.aem.umn.edu/Solid-Liquid_Flows*) (2000).

32 R. A. Gore and C. T. Crowe. Effect of Particle Size on Modulating Turbulent Intensity, *Int. J. Multiphase Flow* **16**, 279 (1989).

33 K. Gustafson and R. Hartman. Divergence-free bases for finite element schemes in hydrodynamics. *SIAM J. Numer. Anal.,* **20**(4):697-721 (1983).

34 C. A. Hall, J. S. Peterson, T. A. Porsching, and F. R. Sledge. The dual variable method for finite element discretizations of Navier-Stokes equations. *Intl. J. Numer. Meth. Engg.,* **21**:883-898, 1985.

35 P. Hansbo. The Characteristic Streamline Diffusion Method for the Time-Dependent Incompressible Navier-Stokes Equations, Comp. *Meth. Appl. Mech. Eng*. **99**, 171–186 (1992).

36 K. Hofler, M. Muller, S. Schwarzer, B. Wachman. Interacting particle-liquid systems, *High Performance Computing in Science and Engineering*, E. Krause and W. Jager, eds., Springer-Verlag, Berlin, 54-64 (1998).

37 H. H. Hu. Direct Simulation of Flows of Solid-Liquid Mixtures, *Int. J. Multiphase Flow* **22**, 335–352 (1996)a.

38 H. H. Hu. Numerical Simulation of Channel Poiseuille Flow of Solid-Liquid Mixtures, in *Proceedings of the Fluids Engineering Division Summer Meeting,* American Society of Mechanical Engineers, **236**, 97–103 (1996)b.

38.a H.H. Hu, N.A. Patankar, and M.Y. Zhu. Direct numerical simulations of fluid-solid systems, to appear in *J. Computational Physics* (2000).

39 H. H. Hu, D. D. Joseph, and M. J. Crochet. Direct Simulation of Fluid Particle Motions, *Theor. Comp. Fluid Dyn.* **3**, 285 (1992).

40 P. Y. Huang, J. Feng, H. H. Hu, and D. D. Joseph. Direct Simulation of the Motion of Solid Particles in Couette and Poiseuille Flows of Viscoelastic Fluids, *J. Fluid Mech*. **343**, 73–94 (1997).

41 P. Y. Huang, J. Feng, and D. D. Joseph. The Turning Couples on an Elliptic Particle Settling in a Vertical Channel, *J. Fluid Mech*. **271**, 1–16 (1994).

42 P. Y. Huang, H. H. Hu, and D. D. Joseph. Direct Simulation of the Sedimentation of Elliptic Particles in Oldroyd B Fluids, *J. Fluid Mech.* **362**, 297–326 (1998).

43 P.Y. Huang and D.D. Joseph. Effects of shear thinning on migration of neutrally buoyant articles in pressure driven flow of Newtonian and viscoelastic fluid, *J. Non-Newtonian Fluid Mech.,* accepted (2000).

44 A. Huerta and W. K. Liu. Viscous Flow with Large Free Surface Motion, Comp. *Meth. Appl. Mech. Eng.* **69**, 227–324 (1988).

45 M. Ishii. *Thermo-Fluid Dynamic Theory of Two-Phase Flows.* Eyrolles, Paris (1975).

46 R. Jackson. Locally averaged equations of motion for a mixture of identical spherical particles and a Newtonian fluid. *Chem. Eng. Sci.* **52**, 2457 (1997)

47 A. Johnson and T. E. Tezduyar. Simulation of Multiple Spheres Falling in a Liquid-Filled Tube, *Comp. Meth. Appl. Mech. Eng*. **134**, 351–373 (1996).

48 A. Johnson & T.E. Tezduyar. 3D simulation of fluid-particle interactions with the number of particles reaching 100. *Comput. Methods Appl. Mech. Engrg.* **145**, 301-321 (1997).

49 A. Johnson & T.E. Tezduyar. Advanced mesh generation and update methods for 3D flow simulations, *Computational Mech.* **23**, 130-143 (1999).

50 D.D. Joseph. Interrogation of Direct Numerical Simulation of Solid-Liquid Flow, to appear (see : *http://www.aem.umn.edu/Solid-Liquid_Flows*) (2000).

51 D. D. Joseph and J. Feng. A Note on the Forces that Move Particles in a Second Order Fluid, *J. Non-Newt. Fluid Mech*. **64**, 299–302 (1996).

52 D. D. Joseph and Y. J. Liu, Motion of Particles Settling in a Viscoelastic Liquid, in *Proceedings of the Second International Congress on Multiphase Flow*, (A. Serizawa, T. Fukano, and J. Bataille, eds.), 3–7 (1995).

53 D.D. Joseph and T.S. Lundgren. Ensemble averaged and mixture theory equations for incompressible fluid-particle suspensions, *Int. J. Multiphase Flow* **16**, 35 (1990).

54 L. R. Kern, T. K. Perkins, and R. E. Wyant. The Mechanics of Sand Movement in Fracturing, Petroleum Transactions, *AIME* **216**, 403–405 (1959).

55 S. Kim and S.J. Karrila. *Microhydrodynamics: Principles and Selected Applications*, Butterworth-Heinemann, Boston (1991).

56 M. G. Knepley, V. Sarin, and A. H. Sameh. Parallel simulation of particulate flows. In *Proceedings of the Fifth International Symposium on Solving Irregular Structured Problems in Parallel*, volume 1457, pages 226-237. Lecture Notes in Computer Science, Springer-Verlag (1998).

57 A. Kuethe and C.Y. Chow. *Foundations of Aerodynamics, 5th Ed*. John Wiley & Sons (1998).

58 A.J.C. Ladd. Sedimentation of homogeneous suspensions of non-Brownian spheres, *Phys. Fluids.* **9**, 491 (1997).

59 D.T. Leighton and A. Acrivos. The Lift on a Small Sphere Touching a Plane in the Presence of a Simple Shear Flow, Z. Angew. *Math. Phys* **36**, 174–178 (1985).

60 D.T. Leighton and A. Acrivos. The shear-induced migration of particles in concentrated suspensions, *J. Fluid Mech.* **181**, 415-439 (1987).

61 Y. J. Liu and D. D. Joseph. Sedimentation of Particles in Polymer Solution, *J. Fluid Mech*. **48**, 225–235 (1993).

61.a B. Maury. A many-body lubrication model, *C.R. Acad. Sci. Paris, T.* **325**, Series 1, 1053-1058 (1999).

62 M.R. Maxey and J.J. Riley. Equation of Motion for a Small Rigid Sphere in a Nonuniform Flow, *Phys. Fluids A* **26**, 883 (1983).

63 J.B. McLaughlin. Inertial migration of a small sphere in linear shear flows, *J. Fluid Mech*., **224**, 261-274 (1991).

64 J.B. McLaughlin. Numerical computation of particle-turbulent interaction, *Int. J. Multiphase Flow* **20**, 211-232 (1994).

65 K. G. Nolte. Fluid Flow Considerations in Hydraulic Fracturing, *SPE* 18537 (1988). See also Errata submitted July 1992 for SPE 18537, available from SPE Book Order Department.

66 T. Nomura and T. J. R. Hughes. An Arbitrary Lagrangian-Eulerian Finite Element Method for Interaction of Fluid and a Rigid Body, Comp. *Meth. Appl. Mech. Eng*. **95**, 115–138 (1992).

67 P.R. Nott and J.F. Brady. Pressure-driven flow of suspensions: Simulations and theory, *J. Fluid Mech.* **275**, 157-199 (1994).

68 P. Oswald. An optimal multilevel preconditioner for solenoidal approximations of the two-dimensional stokes problem. *IMA J. Numer. Anal.,* **18**:207-228, 1998.

69 T.-W. Pan, V. Sarin, R. Glowinski, A. H. Sameh, and J. P'eriaux. A fictitious domain method with distributed Lagrange multipilers for the numerical simulation of particulate flow and its parallel implementation. In *Proceedings of the 10th Parallel CFD Conference*, Aug. 1998.

70 T.Y. Pan, V. Sarin, D.D. Joseph, R. Glowinski and R. Bai. Fluidization of 1204 spheres in a slit bed. To appear (see : *http://www.aem.umn.edu/Solid-Liquid_Flows*) (2000).

71 N. Patankar, P.Y. Huang, T. Ko and D.D. Joseph. Lift-off of a single particle in Newtonian and viscoelastic fluids by direct numerical simulation. To appear (see : *http://www.aem.umn.edu/Solid-Liquid_Flows*) (2000).

72 N.A. Patankar and D.D. Joseph. Lagrangian numerical simulation of particulate flows. *Int. J. Multiphase Flow,* in review (1999).

73 N.A. Patankar and D.D. Joseph. Modeling and numerical simulation of particulate flows by the Eulerian-Lagranian approach, submitted, *Int. J. Multiphase Flow* (2000).

74 N.A. Patankar, P. Singh, D.D. Joseph, R. Glowinski and T.-W. Pan. A new formulation of the distributed Lagrange multiplier/fictitious domain method for particulate flows, *Int. J. Multiphase Flow,* accepted (1999).

75 R.J. Phillips, R.C. Armstrong, R.A. Brown, A.L. Graham and J.R. Abbot. A constitutive equation for concentrated suspensions that accounts for shear-induced particle migration, *Phys. Fluids A*, **4**, 30-40 (1992).

76 D. Qi. Lattice-Boltzmann simulations of particles in non-zero-Reynolds-number flows, *J. of Fluid Mech.* **385,** 41 (25 April 1999)

77 J. F. Richardson and W. N. Zaki. Sedimentation and Fluidization: Part I, *Trans. Instn. Chem.* Engrs*.* **3**2, 35–53 (1954).

78 T. Rusten and R. Winther. A preconditioned iterative method for saddle-point problems. *SIAM J. Matrix Anal. Appl.,* **13**(3):887-904 (1992).

79 P.G. Saffman. On the motion of small spheroidal particles in a viscous liquid*, J. Fluid Mech.* **1,** pp. 540-543 (1956).

80 P.G. Saffman. The lift on a small sphere in a slow shear flow, *J. Fluid Mech.* **22**, 385 (1965).

81 V. Sarin. *Efficient Iterative Methods for Saddle Point Problems.* PhD thesis, University of Illinois, Urbana-Champaign (1997).

82 V. Sarin. Optimal parallel preconditioners for 3d particulate flows. In *Proceedings of the Ninth SIAM Conference on Parallel Processing for Scientific Computing*, Mar. 1999.

83 V. Sarin and A. H. Sameh. An efficient iterative method for the generalized Stokes problem. *SIAM Journal of Scientific Computing,* **19**(1):206-226 (1998).

84 V. Sarin and A. H. Sameh. Large scale simulation of particulate flows. In *Proceedings of the Second Merged Symposium IPPS/SPDP*, pages 660-666, Apr. 1999.

85 J.A Schonberg and E.J. Hinch. Inertial migration of a sphere in Poiseuille flow, *J. Fluid Mech*. **203**, 517 (1989).

86 G. Segré and A. Silberberg. Radial Poiseulle flow of suspensions, *Nature,* **189**, 209 (1961).

87 G. Segré and A. Silberberg. Behaviour of macroscopic rigid spheres in Poiseuille flow, Part I, *J. Fluid Mech.,* **14**, 115 (1962).

88 D. Silvester and A. Wathen. Fast iterative solution of stabilised Stokes systems Part 2: Using general block preconditioners. *SIAM J. Numer. Anal.,* **31**(5):1352-1367 (1994).

89 P. Singh, P. H. Caussignac, A. Fortes, D.D. Joseph, and T. S. Lundgren. Stability of Periodic Arrays of Cylinders Across the Stream by Direct Simulation, *J. Fluid Mech.* **205**, 553–571 (1989).

90 P. Singh, D.D. Joseph, T. Hesla, R. Glowinski and T.-W. Pan. A distributed Lagrange multiplier/fictitious domain model for viscoelastic particulate flows, *J. Non-Newtonian Fluid Mechanics*, accepted for publication (1999).

91 P. Singh and L. G. Leal. Computational Studies of the FENE Dumbbell Model in a Co-Rotating Two-Roll Mill, *J. Rheology* **38**(3), 485–517 (1994).
92 D.M. Snider, P.J. O'Rourke & M.J. Andrews. Sediment flow in inclined vessels calculated using a multiphase particle-in-cell model for dense particle flows, *Int. J. Multiphase Flow* **24**, 1359-1382 (1998)
93 T.E. Tezduyar, J. Liou, M. Behr and S. Mittal. A new strategy for finite element computations involving moving boundaries and interfaces - the DSD/ST procedure: II. Computation of free-surface flows, two-liquid flows, and flows with drafting cylinders. *Comput. Meths. Appl. Mech. Engrg.* **94**, 353-371 (1992).
94 P. Vasseur and R.G. Cox. The lateral migration of a spherical particle in two-dimensional shear flows, *J. Fluid Mech.* **78**, 385 (1976).
95 A. Wathen and D. Silvester. Fast iterative solution of stabilised Stokes systems Part 1: Using simple diagonal preconditioners. *SIAM J. Numer. Anal.,* **30**(3):630-649 (1993).
96 D.Z. Zhang, & A. Prosperetti. Averaged equations for inviscid disperse two-phase flow, *J. Fluid Mech*. **267**, 185-219 (1994).
97 D.Z. Zhang and A. Prosperetti. Momentum and energy equations for disperse two-phase flows and their closure for dilute suspensions, *Int. J. Multiphase Flow* **23**, 425 (1997).